Journal of Pharmaceutical Analysis 8 (2018) 413–420

Contents lists available at ScienceDirect

Journal of Pharmaceutical Analysis

journal homepage: www.elsevier.com/locate/jpa
www.sciencedirect.com

Original Research Article

Novel ligand-based docking; molecular dynamic simulations; and absorption, distribution, metabolism, and excretion approach to analyzing potential acetylcholinesterase inhibitors for Alzheimer's disease

Subramaniyan Vijayakumar [a,*], Palani Manogar [a], Srinivasan Prabhu [a], Ram Avadhar Sanjeevkumar Singh [b]

[a] Computational Phytochemistry Laboratory, PG and Research Department of Botany and Microbiology, AVVM Sri Pushpam College (Autonomous) Poondi, Thanjavur (Dist), Tamil Nadu, India
[b] Computer Aided Drug Design and Molecular Modeling Laboratory, Department of Bioinformatics, Alagappa University, Karaikudi 630004, Tamil Nadu, India

ARTICLE INFO

Article history:
Received 2 March 2017
Received in revised form
12 July 2017
Accepted 13 July 2017
Available online 14 July 2017

Keywords:
Alzheimer's disease
Acetylcholinesterase
Phytocompounds
Molecular docking
Free energy calculations
Molecular dynamic simulations

ABSTRACT

Acetylcholinesterase (AChE) plays an important role in Alzheimer's disease (AD). The excessive activity of AChE causes various neuronal problems, particularly dementia and neuronal cell deaths. Generally, anti-AChE drugs induce some serious neuronal side effects in humans. Therefore, this study sought to identify alternative drug molecules from natural products with fewer side effects than those of conventional drugs for treating AD. To achieve this, we developed computational methods for predicting drug and target binding affinities using the Schrodinger suite. The target and ligand molecules were retrieved from established databases. The target enzyme has 539 amino acid residues in its sequence alignment. Ligand molecules of 20 bioactive molecules were obtained from different kinds of plants, after which we performed critical analyses such as molecular docking; molecular dynamic (MD) simulations; and absorption, distribution, metabolism, and excretion (ADME) analysis. In the docking studies, the natural compound rutin showed a superior docking score of −12.335 with a good binding energy value of −73.313 kcal/mol. Based on these findings, rutin and the target complex was used to perform MD simulations to analyze rutin stability at 30 ns. In conclusion, our study demonstrates that rutin is a superior drug candidate for AD. Therefore, we propose that this molecule is worth further investigation using in vitro studies.

1. Introduction

Alzheimer's disease (AD) is an irreversible neurodegenerative disease of brain neurons. The term Alzheimer's was first used by the German physician Alois Alzheimer in 1906 [1]. According to the World Health Organization (WHO), AD is the commonest cause of dementia, and it affects approximately 25 million people worldwide [2]. Acetylcholine (ACh) is an organic substance involved in the transfer of neuronal signals in the brain. Its hydrolysis into a cholineacetyl group is catalyzed by acetylcholinesterase (AChE) [3], which is a well-known enzyme that plays an important role in the central nervous system (CNS) [4]. The most important etiological factor in AD is not yet known; however, some established abnormal brain pathologies such as AChE over-expression and extracellular accumulation of "mysterious" β-amyloid plaques are the trademark of this disease.

Currently, four drugs that act as inhibitors of AChE are used in patients with AD, which are tacrine, dopenzial, galantamine, and rivastigmine [5–8]. These drugs are known to induce several side effects such as gastrointestinal disturbances, and they have low bioavailability. Hence, it is urgent to develop better inhibitors of AChE from natural sources to treat AD without any side effects. Currently, plants are used to enhance memory and to alleviate other problems associated with AD. Natural products and their derivatives are known to have efficient biological activities against numerous diseases, including CNS disorders [9]. Numerous plant-derived substances that may be considered as potential AChE drug molecules belong to different classes of compounds characterized by their structures [10].

Generally, medicinal plant-derived secondary metabolites such as alkaloids, flavonoids, tannins, saponins, and other phytochemicals show promising activities when they are consumed. They are also produced as part of the defence mechanisms against various

Peer review under responsibility of Xi'an Jiaotong University.
* Corresponding author.
E-mail address: svijaya_kumar2579@rediff.com (S. Vijayakumar).

https://doi.org/10.1016/j.jpha.2017.07.006

disorders and some highly pathogenic diseases. These active substances have been found to be beneficial for numerous therapeutic uses [11]. Recently, numerous plant-derived drugs have been investigated in clinical phase trials, and the trials of some molecules against globally challenging diseases have been successfully completed [12].

Currently, patients are seeking plant-based drug treatments for their health needs because these drugs are believed to have fewer side effects. Most individuals take only crude extracts for their health complaints which can never let them know the scientific background. Many research studies have isolated bioactive compounds from natural sources, but comprehensive studies are required to determine their molecular interactions. Therefore, in this study, we investigated the efficacy of some bioactive molecules using molecular docking and confirmed their mode of interaction with AChE.

2. Tools and methods

2.1. Modeling platform

The entire computational analysis was carried out using the Schrodinger suite using the Maestro10.2 version packages including LigPrep, Glide XP docking, grid generation, free energy calculations, absorption, distribution, metabolism, and excretion (ADME) toxicity, and MD simulations. Centos Linux was used as the operating system.

2.2. Biological data

In this study, 20 bioactive molecules were retrieved from the chemical database [13]. The AChE target was taken from the Protein Data Bank [14], and its databank alpha-numeric identity is PDB: 1B41.

2.3. Preparation of the protein

The protein was prepared using the wizard tool in Maestro version 10.2. During the process, the missing side and back chains were included [15]. The tool has two gears, namely, preparation and refinement. The X-ray crystallography structure of the protein molecules was occasionally bound and tangled with water molecules. The water molecule occupying the protein structure was not suitable for the docking study and, therefore, it was removed. Finally, the optimization and minimization processes were completed in this step [16].

2.4. Ligand preparation

All the ligand molecules were prepared using LigPrep2.4 [17], which can generate a number of structures from each input structure with various ionization states, tautomers, stereochemical characteristics, and ring conformations to eliminate molecules on the basis of various criteria such as molecular weight or specified numbers and types of functional groups with correct chiralities for each successfully processed input structure. The OPLS 2005 force field was used for the optimization, which produced the low-energy isomer of the ligand [18]. Finally, all the ligand molecules formed in the complex structure for input were docked.

2.5. Molecular docking

First, to test the docking parameters, all the ligand molecules were docked into the binding site of AChE using the Grid glide-based ligand docking program of Schrödinger suite [19,20]. In this study, the Maestro10.2 version tool was used to perform rigid, flexible docking for predicting the binding affinity, ligand efficiency, and inhibitory constant to the target [21]. The ligands were docked to the active site of AChE using Glide Extra precision (XP), which docks to determine the ligand's flexibility. Only the active small molecule would have available access to avoid the penalties and receive favourable docking scores with accurate hydrophobic contact between the protein and ligand. The electrostatic energy interaction of the hydrogen bonds involved both the side and back chains, hydrophobic contact, and Salt bridge contacts [22].

2.6. MD simulation

MD simulations were carried out using the Desmond software [23,24]. The optimized potentials for the liquid simulations (OPLS)-2005 force field were used in this system to determine the protein (AChE) interactions with efficient ligand molecules, which was solvated with the simple point charged (TIP4P) water model [23]. The orthorhombic water box was used to create a 10 Å buffer region between the protein atoms and box sides. Overlapping water molecules were deleted, and the systems were neutralized with Na^+ ions. The OPLS-2005 force field was used for energy calculation. The temperature was maintained constant at 300 K, and a 2.0 fs value was obtained in the integration step. We executed MD simulations for the complex structure of the protein as well as the target with position restraints for 6000 ps to allow the water molecules to remain in the system. Finally, the root mean square deviation (RMSD) was calculated to monitor the stability of the AChE protein in its native motion. The synchronize file was saved every 5000 ps for up to 30 ns and the result was scrutinized using the method described by Nagasundaram et al. [25].

2.7. Prime molecular mechanics-generalized born surface area (MM-GBSA) calculations

The ligand binding energy of each of the 20 phytocompounds required to inhibit AChE was estimated using the prime molecular mechanics-generalized born surface area (MM-GBSA) module in the Schrodinger Suite 2014 [26,27]. The total free energy binding (digibind, kcal/mol) was estimated as follows using the software:

$$\Delta G_{bind} = G_{complex} - \left(G_{protein} + G_{ligand}\right)$$

Where each energy term is a combination of G=molecular mechanics energies (MME)+GSGB (SGB solvation model for polar solvation)+GNP (non-polar solvation) [28] coulomb energy, covalent binding energy, Vander Waals energy, lipophilic energy, GB electrostatic solvation energy, prime energy, hydrogen-bonding energy, hydrophobic contact, and self-contact correction [29]. We then used this score to rank the ligand-protein Glide XP docked complex.

2.8. ADME toxicity

This approach has been very useful in drug discovery, especially in determining the mechanism of action of molecules [30]. A set of ADME-related properties was calculated for each of the 20 natural compounds using the QikProp program (Schrödinger software), which was run in the normal mode. QikProp generates physically relevant descriptors, and the toxicity of a ligand is considered important for it to act as an effective drug in new drug development [31,32].

3. Results and discussion

3.1. Molecular docking simulations and validation of docking protocol

The current study aimed to exploring the excessive activity of AChE inhibition bioactive molecules. The AChE target had a sequence length of 539 amino acids with a resolution of 2.76 Å. Descriptive hydrogen atoms were added to all the inhibitors to ensure they had all-atom structures, followed by energy minimization. After the preparation process, the protein was ready for molecular docking. This procedure shows the potential of the drug molecules to bind with the protein pocket and their hydrogen bond interactions. The complexes of each of the 20 bioactive molecules docked with the AChE protein. The molecular docking method has produced ligand docking scores with generating their H-bond distance values between ligand and target, and the consequent glide energy was also generated.

In this computational analysis, rutin had a higher docking score than that of the other ligand molecules. Furthermore, it showed a better binding affinity for the target than the other small molecules did. The bioactive molecule of rutin comes under the groups of flavonoids, and it has also exhibited admirable pharmacological and biological activities in numerous experimental studies. Recently, Ganeshpurkar and Saluja [33] reported that rutin shows effective pharmacological potential against the majority of diseases and conditions including neuroinflammation, and it promotes neuralcrest cell survival and has sedative, anticonvulsant, and anti-AD activities. Furthermore, it has been used in treatment of conditions such as hyperkinetic movement disorder, depression, and stroke.

In the present study, most of the bioactive molecules exhibited docking scores above −9.0 Among them, rutin had a superior docking score of −12.335, followed by hesperidin, which had a score of −10.708. At the end of this analysis, the computational tool showed some important outputs such as the ligand glide energy value and the MM-GBSA calculations (Table 1). Recently, numerous studies have used the molecular docking method because it identifies suitable drug molecules for the target of interest [34–36]. In this study, the phytocompounds showed good measurable binding affinities for the target residues. The binding affinities were indicative of the ligand's contribution to and flexibility for the target. The present study also showed the H-bond distances and their contacts types for each molecule.

3.1.1. Rutin

The AChE protein residues interacted with the ligand atoms, and the surfaces were controlled by a complex array of intermolecular interactions. Such interactions depend on both specific interactions at the bindings site and the non-specific forces outside the target binding pocket. Here, the pattern of interaction between AChE and rutin in the complex is shown. We examined the site at which rutin bound to the target and found that it robustly interacted with the AChE residue to form a hydrogen bond. The Asp264, Asn564, His436, Arg327, Pro399, and Glu344 residues were in contact with the ligand atoms. Furthermore, Pro399 formed covalent hydrogen back chain contacts. Asn 264 formed H-bond back chain contacts with the rutin molecule. Arg327, Asn564, His436, and Glu344 formed H-bond side chain contacts with the ligand. His436 formed contacts with the side chain and π-π stacking contacts with rutin. It had a superior docking score to that of the other bioactive molecules, which is shown in Table 1. The ligand molecule residue contacts, hydrogen bond distances, and the types of contacts are shown in Fig. 1.

3.1.2. Hesperidin

Among the 20 ligands, hesperidin showed a docking score that was close to that of rutin at −10.708, and its glide energy values are shown in Table 1. The docked complex was examined, and the residue contacts with the ligand atoms were observed. The interaction plot shows the residue interactions of Thr269, Asp264, Gly265, Arg327, His436, and Pro399. The contacts formed involved different kinds of bonding lines and were back and side chain contacts, as well as hydrophobic contacts with rutin. Complete residues were formed only with the H-bond back chain contacts, except for the His436 residues because it connected the π-π stacking contacts with the ligand. The scrutinized docked complex

Table 1
Docking results of 20 bioactive molecules (ligands) and the energy generated by the active site of acetylcholinesterase (AChE).

S. no.	Compound name	Glide XP docking score	Glide XP energy (kcal/mol)	Glide XP emodel	MM-GBSA d Gbind (kcal/mol)
1.	Rutin	−12.335	−76.583	−90.567	−73.313
2.	Hesperidin	−10.708	−65.317	−85.199	−76.888
3.	5-O-[(2E)-3-(4-hydroxyphenyl)2-propenoyl]pentofuranosyl-(1–3)pentopyranosyl-(1–4)pentose	−10.512	−61.189	−63.749	−64.286
4.	Narirutin	−10.121	−61.981	−57.486	−65.786
5.	Glycyrrhizin	−9.954	−76.800	−61.064	−71.220
6.	Procyanidin B2	−9.691	−57.812	−78.705	−69.145
7.	Chlorogenic acid	−9.568	−50.985	−58.412	−64.789
8.	Zanamivir	−9.534	−48.060	−52.536	−52.115
9.	Mangiferin	−9.445	−51.920	−32.795	−50.071
10.	(R)-(+)-rosmarinic acid	−9.101	−54.367	−52.925	−54.433
11.	Ecdysterone	−7.786	−45.813	−55.997	−58.151
12.	D-(+)-Catechin	−6.944	−37.972	−50.899	−74.389
13.	D-(-)-Mannitol	−6.835	−34.461		−40.552
14.	Cidofovir	−6.744	−43.076	−46.260	−42.374
15.	rac 8-Prenylnaringenin	−6.584	−46.158	−42.355	−57.609
16.	Epicatechin	−6.582	−36.594	−55.853	−57.653
17.	(-)-Andrographolide	−6.324	−34.059	−51.453	−58.033
18.	Trifluridine	−6.276	−33.924	−42.160	−55.218
19.	(+)-[6]-Gingerol	−6.192	−40.933	−60.933	−41.552
20.	3-hydroxy-2,3-dihydropyrrolo[2,1b]quinazolin-9(1H)-one	−6.163	−50.509	−55.345	−58.090

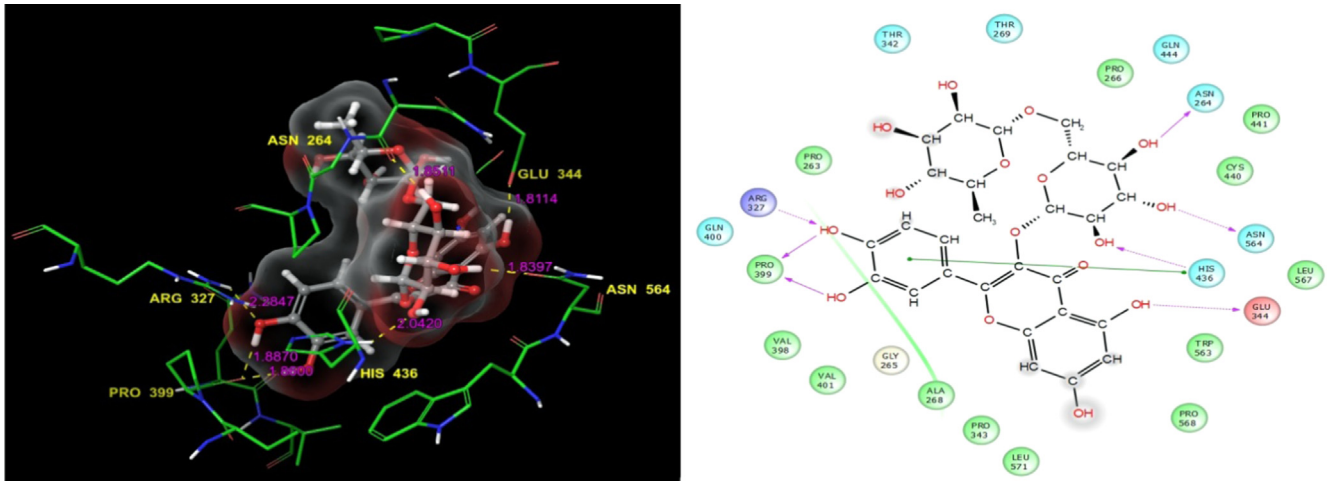

Fig. 1. Rutin: Residues and hydrogen bond contacts (yellow dotted line) with their distance values (pink values), and the 2D template representing the types of contacts formed between the ligand and target.

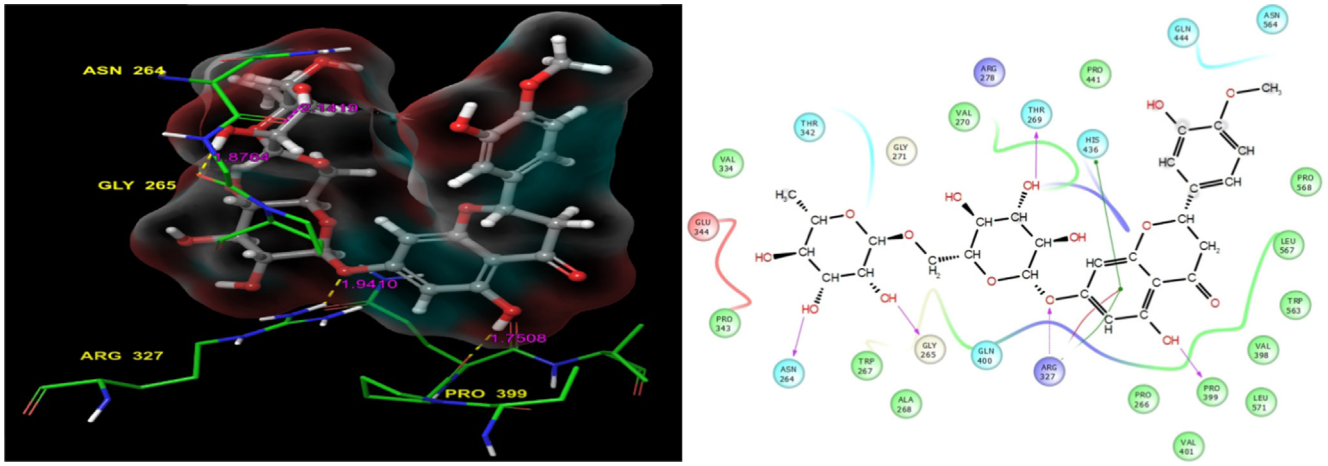

Fig. 2. Hesperidin: Residues and hydrogen bond contacts (yellow dotted line) with their distance values (pink values), and the 2D template representing the types of contacts formed between the ligand and target.

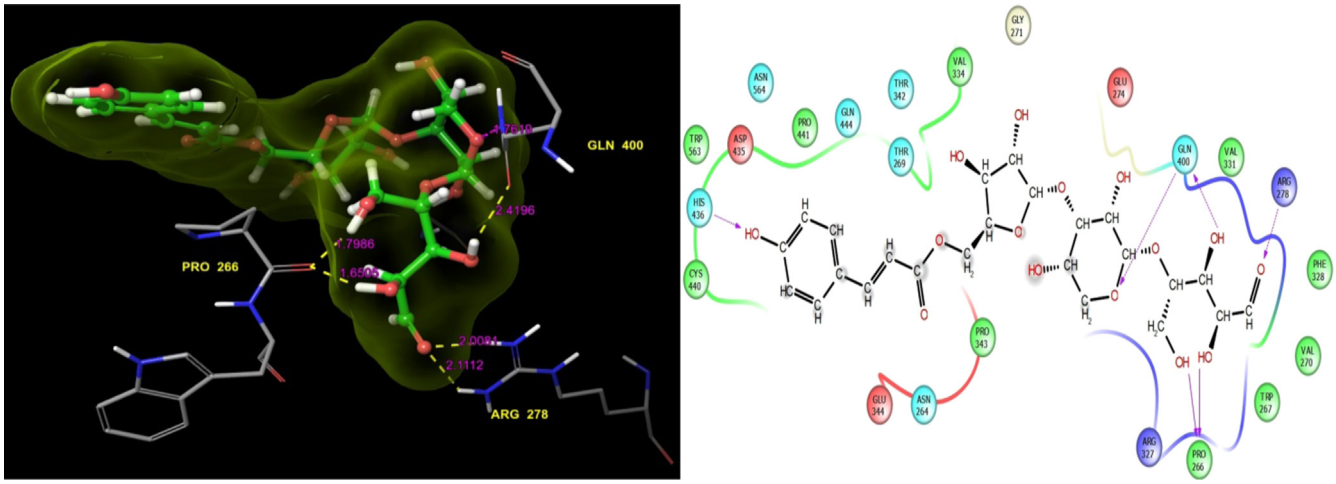

Fig. 3. 5-O-[(2E)-3-(4-hydroxyphenyl)2-propenoyl]pentofuranosyl-(1-3)pentopyranosyl-(1-4)pentose: Residues and hydrogen bond contacts (yellow dotted line) with their distance values (pink values), and the 2D template representing the types of contacts formed between the ligand and target.

details such as the H-bond distance values, and the types of contacts are shown in Fig. 2. Previously, Remya et al. [37] conducted molecular docking studies of AChE using bioactive molecules, which showed that the hesperidin molecule had good binding affinities for AChE. It also had the second highest docking score in this study, similar to the results of this computational analysis. In addition, the anticoagulant activity of hesperidin has been investigated in vitro studies [37,38].

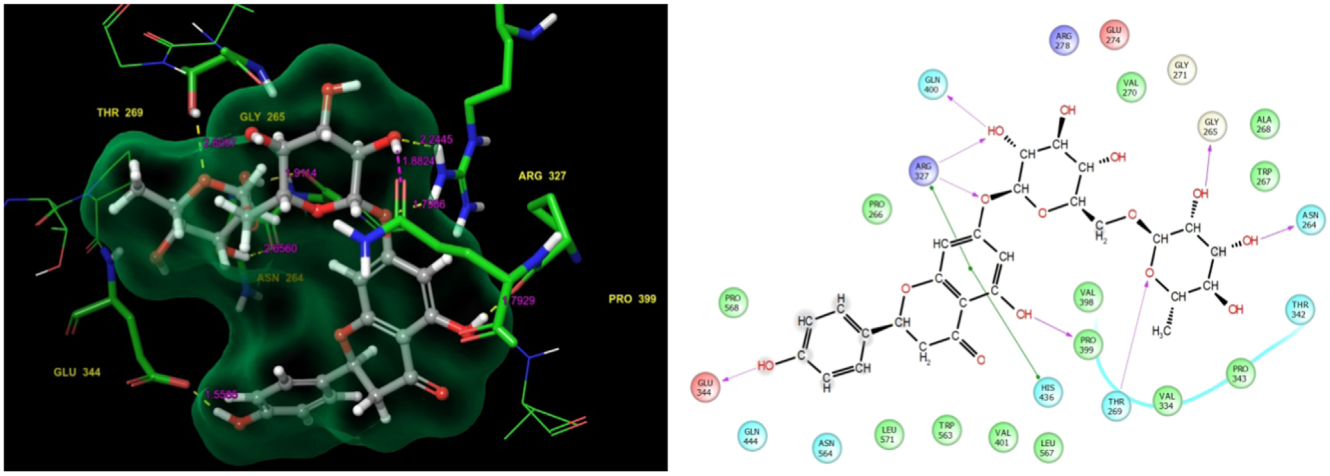

Fig. 4. Narirutin: Residues and hydrogen bond contacts (yellow dotted line) with their distance values (pink values), and the 2D template representing the types of contacts formed between the ligand and target.

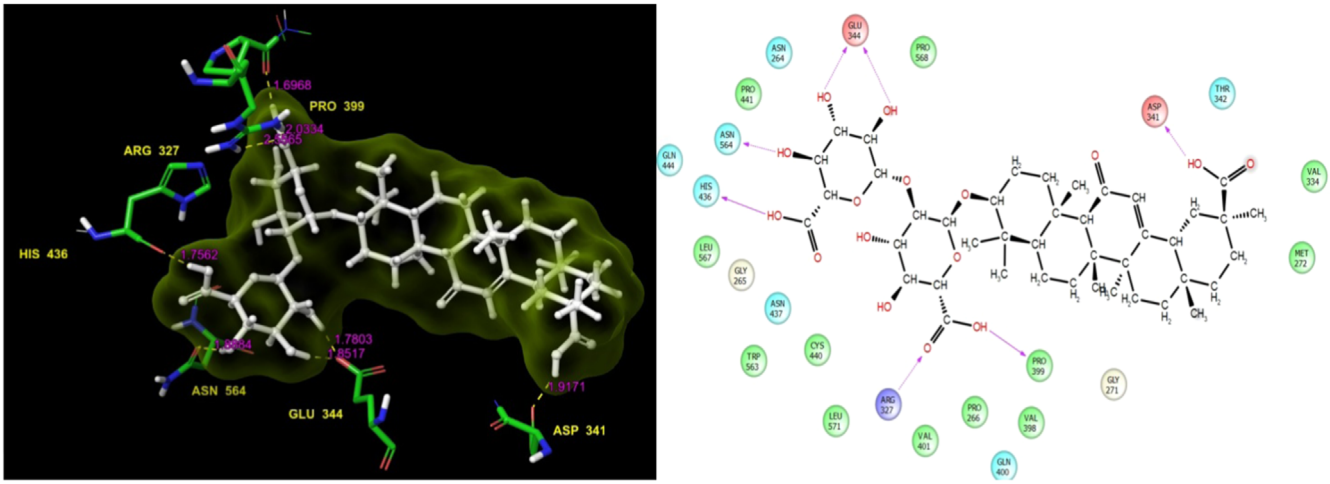

Fig. 5. Glycyrrhizin: Residues and hydrogen bond contacts (yellow dotted line) with their distance values (pink values), and the 2D template representing the types of contacts formed between ligand and target.

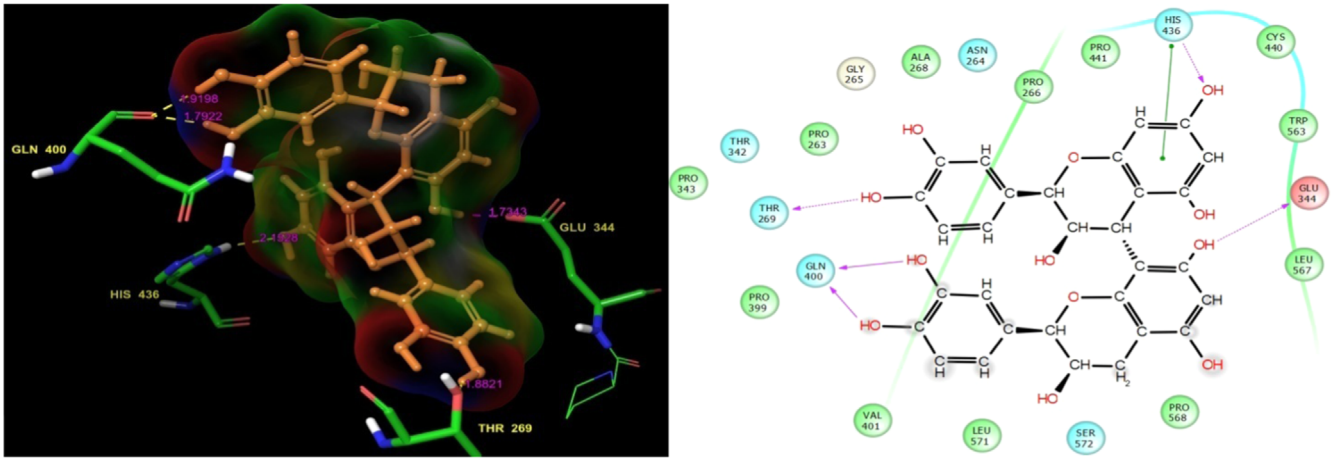

Fig. 6. (+)-Procyanidin B2: Residues and hydrogen bond contacts (yellow dotted line) with their distance values (pink values), and the 2D template representing the types of contacts formed between the ligand and target.

3.1.3. 5-O-[(2E)-3-(4-hydroxyphenyl)2-propenoyl]pentofuranosyl-(1-3)pentopyranosyl-(1-3.5.4)pentos

The bioactive molecular 5-O-[(2E)-3-(4-hydroxyphenyl)2-propenoyl]pentofuranosyl-(1-3)pentopyranosyl-(1-3.5.4)pentose showed the third most valuable docking score (−10.512) with good glide energy value (Table 1). The docked complex examination showed the residue was in contact with the ligand. His436, Gln400, and Pro266 formed H-bond back and side chain contacts

Table 2
Acetylcholinesterase (AChE) enzyme residue contacts with 20 bioactive molecules.

S. no.	Phytocompounds	Residues interactions and their distances	Types of bond formation	
			H-bond back chain	H-bond side chain
1.	Rutin	Pro 399 (1.86, 1.88), Arg 327 (2.28), Glu 344 (1.81), Asn 264 (1.85), Asn 564 (1.83), His 436(2.04)	Arg 327, Glu 344, Asn 564, His 436	Pro 399, Asn 264
2.	Hesperidin	Pro 399 (1.75), Asn 264 (2.14), Gly 265(1.87), Arg (1.94)	Arg 327 (1.94)	Pro 399 (1.75), Asn 264 (2.14), Gly 265 (1.87),
3.	5-O-[(2E)-3-(4-Hydroxyphenyl) 2-propenoyl]pentofuranosyl-(1–3) pentopyranosyl-(1–4)pentose	Pro 266 (1.65), (1.79), Arg 278 (2.11, 2.08), Glu 400 (2.41), His 436 (2.44)	Pro 266 (1.65)	Arg 278, Glu 400, His 436
4.	Narirutin	Glu 344 (1.55), Gln 400 (1.88), Gly 265 (1.91), Asn 264 (2.65), Thr 296 (2.60) and Pro 399 (1.79)	Glu 344, Gln 400, Gly 265, Thr 269	Asn 264, Pro 399
5.	Glycyrrhizin	Glu 344 (1.85), Asp 341(1.78), Asn 564 (1.88), His 436 (1.75), Arg 327 (2.55, 2.03), Pro 399(1.69)	Glu 344, Asp 341, Asn 564, Arg 327	His 436, Pro 399
6.	(+)-ProcyanidinB2	Gln 400 (1.79), Thr 269 (1.92), Glu 344 (1.23), His 436 (2.75)	Thr 269, Glu 344, His 436	Gln 400
7.	Chlorogenic acid	Asn 564 (1.85), Asn 264 (1.94), His 436 (1.89, 1.94), Pro 399 (2.03), Glu 344 (2.15)	Asn 564, His 436, Glu 344	Asn 264, Pro 399
8.	Zanamivir	His 436 (2.14), Asn 564 (2.21), Asn 264 (1.87), Glu 344 (1.92, 1.98), Gln 444 (1.78)	His 436, Asn 564, Asn 264, Glu 344	Gln 444
9.	Mangiferin	Gln 444 (1.63), Asn 564 (1.79), Thr 269 (1.93), Gln 400 (2.15)	Gln 444, Asn 564, Gln 400	Thr 269
10.	(R)-(+)-rosmarinic acid	Asn 264 (2.04), His 436 (1.95), Asn 564 (1.89), Pro 399 (1.97), Arg 327 (2.49)	Asn 564, Pro 399, Arg 327	Asn 264, His 436
11.	Ecdysterone	Asn 264 (1.88, 2.02), Arg 327 (2.38), Gln 400 (2.21, 2.16)	Arg 327, Gln 400	Asn 264
12.	D-(+)-Catechin	Gln 444 (2.03), Asn 264(2.37), Trp 563(1.63), Pro 399 (1.95)	Asn 264, Trp 563, Pro 399	Gln 444
13.	D-(-)-Mannitol	Glu 344 (1.92), Asn 264 (1.64), Gln 444 (2.14), Asn 564 (2.05)	Glu 344, Gln 444, Asn 564	Asn 264
14	Cidofovir	Pro 399 (2.11), Gln 400 (2.08, 2.04), Asn 564 (1.71), His 476 (1.78, 2.13)	Pro 399, Asn 564, His 476	Gln 400, His 476
15	rac 8-Prenylnaringenin	Asn 564 (1.74), His 436 (2.20), Gln 400 (1.93), Glu 344 (2.03)	Asn 564, His 436, Glu 344	Gln 400
16	Epicatechin	Glu 344 (1.89, 2.11), Asn 564 (1.96), Trp 563 (1.87)	Glu 344, Asn 564	Trp 563
17	(-)-Andrographolide	Asn 564 (1.72, 1.82)	Asn 564	–
18	Trifluridine	His 436 (2.05), Pro 399 (1.85), Arg 327 (1.97)	His 436, Arg 327	Pro 399
19.	(+)-[6]-Gingerol	Arg 327 (2.22, 2.70), Pro 399 (1.88), His 436 (1.95)	Arg 327	Pro 399, His 436
20.	3-Hydroxy-2,3-dihydropyrrolo [2,1-b]quinazolin-9(1H)-one	Glu 163 (1.93)	–	Glu 163

with the ligand. Specifically, the Gln400 residue was covalently bound to the ligand at the side chain contacts, and one end was connected to the ligand oxygen group while the other end was connected to the functional group of the ligand. The remaining Pro266 was covalently bound with the ligand functional group. The ligand molecule residue contacts, hydrogen bond distance values, and the types of contacts are shown in Fig. 3.

3.1.4. *Narirutin*

Narirutin had the fourth highest docking score of −10.121 and its glide energy value is shown in Table 1. It showed good binding affinities with the target residues. The scrutinized docked complex clearly showed the residue contacts. Specifically, Glu344, Gln400, Arg327, Thr269, Gly265, and Asn264 formed contacts with various atoms of narirutin. The interaction plot clearly shows the residue contacts with the side chain, back chain, and π-π stacking. Gly265 and Asn264 formed H-bond back chain contacts. The remaining residues, Glu344, Gln400, Arg327, and Thr269, formed H-bond side chain contacts with narirutin. Arg327 formed covalent H-bond contacts with the ligand. One end was connected to the ligand functional group while the other was an oxygen group. The π-π stacking bond contact formation was also shown. The ligand molecule residue contacts, hydrogen bond distance values, and the types of contacts are shown in Fig. 4. Murata et al. [39] evaluated the biological potential of narirutin, and found that it showed a significantly strong anti-degranulating activity.

3.1.5. *Glycyrrhizin*

Glycyrrhizin showed the fifth highest docking score of −9.954 and a good glide energy value, which was the highest in this study (Table 1). It also showed good binding affinity. The docked complex showed a higher level of residue interactions than did the other ligand interaction patterns in this study. Specifically, Asn564, His436, Glu344, Arg327, Pro399, and Asp341 formed different kinds of H-bond contact lines with glycyrrhizin as well as the target. Asn564, Glu344, Arg327, and Asp341 were involved in the H-bond side chain contacts with glycyrrhizin. The Glu344 residue formed covalent contacts with the functional groups of the ligand and its molecule residue contacts, hydrogen bond distance values, and the types of contacts are shown in Fig. 5.

3.1.6. *(+)-Procyanidin B2*

(+)-Procyanidin B2 had the sixth highest docking score of −9.691 and a good glide energy value (Table 1). However, it showed a lower binding affinity than those of the previously listed small molecules. The docked complex interaction template showed it had residue interactions with Thr269, Gln400, His436, and Glu344. Moreover, Thr269, His436, and Gln344 were involved in side chain contacts with (+)-procyanidinB2 while Gln400 formed H-bond back chain contacts. It was also covalently bound with the functional groups of the ligand. Surprisingly, the His436 residue was involved in the H-bond side chain and π-π stacking contacts. The ligand molecule residue contacts, hydrogen bond distance values, and the types of contacts are shown in Fig. 6. The AChE residue interactions, H-bond distance values, and their contacts are shown in Table 2.

Similar to our study, Shruthika and Jency [40] previously performed molecular docking studies. However, they studied bioactive molecules against AD targets. They also screened 13 bioactive

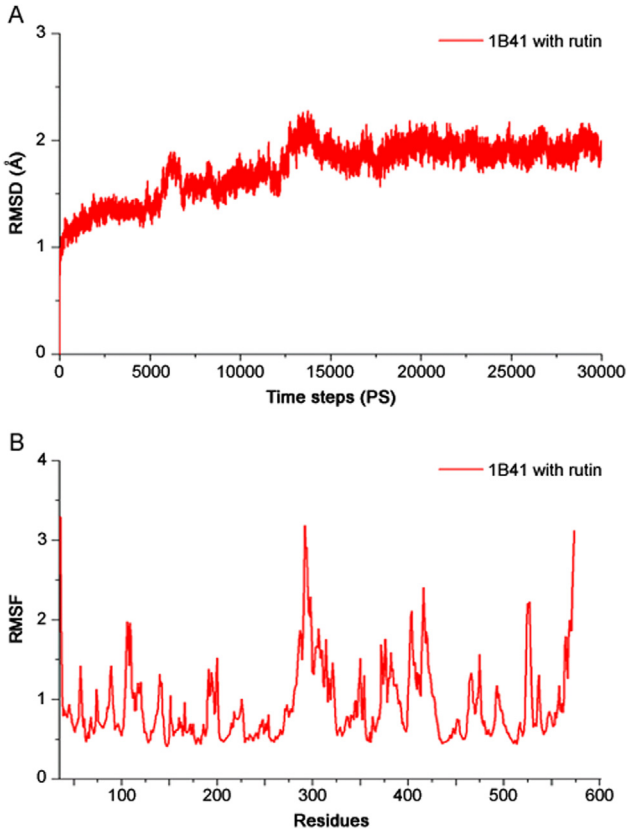

Fig. 7. Molecular dynamic (MD) simulations: (A) Root mean standard deviation (RMSD) of rutin with acetylcholinesterase (AChE) complex as a function of simulation time. (B) Root mean square fluctuation (RMSF) values of complex AChE residues with rutin.

molecules to determine their docking scores, binding energy, and number of bonds formed. Based on their research, the bioactive molecules docked against AChE. However, this research outcome represents bioactive molecules that showed superior docking scores and higher maximum binding affinities than those of the molecules reported previously [40].

3.2. MD

The MD simulation was performed for AChE and rutin complex to evaluate the structural constancy using the Desmond software. We ran MD simulations for the AChE protein and rutin for 30 ns. Initially, the RMSD plot showed that the complex deviated for a certain period and attained equilibrium at 17 ns. Subsequently, it remained stable throughout the simulation time for up to 30 ns (Figs. 7A and B).

3.3. ADME analysis

In this study, the ADME properties of 20 bioactive molecules were analyzed using the QikProp tool. This analysis presents the physicochemical properties of both synthetic and organic molecules and their biological functions. Based on the previous analysis, the physicochemical and biological properties we analyzed included the bioactive molecules, molecular formula, molecular weight, volume, SASA, acceptor H-bond, donor H-bond groups, the number of ring atoms, QPlogPw (−2 to 6.5), percentage human oral absorption, and CNS effects. These are all listed in Table 3. The ADME-based analysis is an important method for analyzing the efficacy of drug molecules. Much more information is recently available from studies related to ADME toxicity analysis of ligands including donor and acceptor hydrogen bonds, QPlogPw, percentage human oral absorption, and molecular weight [39].

4. Conclusion

AChE is one of the vital enzymes involved in regulating neuronal signaling. The excessive activity of this enzyme in patients with AD causes memory loss and impaired cognitive ability. Patients with AD are currently administered synthetic drugs that affect the organs and induce side effects. Therefore, our research study sought to identify alternative drugs from naturally available plants and their products. Of the bioactive molecules we screened, 20 showed potential and were selected. Their activity against the AChE target was analyzed to determine their suitability as drug molecules for treating AD by using computation. Most of the tested ligands exhibited effective docking

Table 3
Physicochemical properties and biological functions of 20 bioactive molecules analyzed using QikProp.

S. no.	Molecular formula	Molecular weight (Da)	Volume	SASA	Acceptor H-bond groups	Donor H-bond groups	Number of ring atoms	QPlogPw (−2 to 6.5)	% Human oral absorption	CNS	Rule of five
1.	$C_{27}H_{30}O_{16}$	610.524	1552.483	778.079	20	9	28	−2.557	0.000	−2	3
2.	$C_{28}H_{34}O_{15}$	610.568	1671.132	866.924	20	7	28	−1.354	0.000	−2	3
3.	$C_{24}H_{32}O_{15}$	560.508	1568.806	821.477	22	7	17	−3.007	0.000	−2	3
4.	$C_{27}H_{32}O_{14}$	580.541	1611.303	837.282	19	7	28	−1.397	0.000	−2	3
5.	$C_{42}H_{62}O_{16}$	822.942	2190.041	1057.957	21	6	34	1.884	0.000	−2	3
6.	$C_{30}H_{26}O_{12}$	578.528	1519.296	807.567	10	10	32	0.453	0.000	−2	3
7.	$C_{16}H_{18}O_{9}$	354.313	995.503	553.076	9	6	12	−0.515	14.088	−2	3
8.	$C_{12}H_{20}N_{4}O_{7}$	332.313	963.976	535.187	12	9	6	−2.426	0.000	−2	1
9.	$C_{19}H_{18}O_{11}$	422.345	1127.265	634.363	13	7	20	−1.760	0.000	−2	2
10.	$C_{18}H_{16}O_{8}$	360.320	1094.899	637.616	7	5	12	−0.957	35.097	−2	2
11.	$C_{27}H_{44}O_{7}$	480.640	1443.524	746.044	9	6	17	−2.223	61.286	−2	0
12.	$C_{15}H_{14}O_{6}$	290.272	856.481	503.931	5	5	16	0.427	61.480	−2	1
13.	$C_{6}H_{14}O_{6}$	182.173	595.353	369.932	10	6	0	−3.079	28.264	−2	0
14.	$C_{8}H_{14}N_{3}O_{6}P$	279.189	794.879	616.277	12	5	6	−1.245	21.969	−2	1
15.	$C_{20}H_{20}O_{5}$	340.375	1093.897	466.636	2	2	16	3.323	88.020	−2	0
16.	$C_{15}H_{14}O_{6}$	290.272	834.190	477.400	5	5	16	0.286	60.152	−2	0
17.	$C_{20}H_{30}O_{5}$	296.203	1041.592	547.798	3	3	15	1.289	78.344	−2	0
18.	$C_{10}H_{11}F_{3}N_{2}O_{5}$	294.390	836.626	516.586	3	3	11	−0.359	53.875	−2	0
19.	$C_{17}H_{26}O_{4}$	234.821	1057.263	587.815	1	1	6	3.561	100.000	−2	0
20.	$C_{6}H_{11}O_{6}$	179.056	1037.142	526.327	6	5	13	−1.693	0.000	−2	0

SASA: Solvent Accessible Surface Area; QPlogPw: Solvation free energy in water; CNS: Central Nervous System.

scores with good binding affinities. In particular, rutin showed a superior docking score to that of the other bioactive molecules against AChE. Based on the outcome, we further evaluated the residue interaction with rutin and found it showed the maximum level of binding affinities. The other promising bioactive molecules, hesperidin, narirutin, glycyrrhizin and (+)-procyanidin B2 also showed good binding affinities in this analysis. Based on these results, we concluded that rutin is an effective and favourable potential anti-AChE drug and it may be a suitable drug candidate for AD. Further, in vitro studies on the purified rutin molecule are ongoing using various concentrations in neuronal cell lines.

Conflicts of interest

The authors declare that there are no conflicts of interest.

Acknowledgments

The authors are grateful to the DST-SERB (SB/YS/LS-109/2014) for providing financial assistance for this project. We especially express our thanks to the management of A.V.V.M. Sri Pushpam College (Autonomous), Poondi, for providing the necessary facilities and support to carry out this work.

References

[1] A.K. Singhal, V. Naithani, O.P. Bangar, Medicinal plants with a potential to treat Alzheimer and associated symptoms, Int. Nutr. Pharmacol. Neurol Dis. 2 (2012) 84–91.
[2] C. Qiu, M. Kivipelto, E. von Strauss, Epidemiology of Alzheimer's disease: occurrence, determinants, and strategies toward intervention, Dialogues Clin. Neurosci. 11 (2009) 111–128.
[3] A. da Silva Goncalves, T.C. Franca, O. Vital de Oliveira, Computational studies of acetylcholinesterase complexed with fullerene derivatives:a new insight for Alzheimer disease treatment, J. Biomol. Struct. Dyn. 34 (2016) 1307–1316.
[4] M.B. Colovic, D.Z. Krstic, T.D. Lazarevis Pasti, Acetylcholinesterase inhibitors: pharmacology and toxicology, Curr. Neuropharmacol. 11 (2013) 315–335.
[5] P.J. Whitehouse, Cholinergic therapy in dementia, Acta Neurol. Scand. Suppl. 149 (1999) 42–45.
[6] C.A. Kelly, R.J. Harvey, H. Cayton, Drug treatments for Alzheimer's disease, Br. Med. J. 314 (1997) 693–694.
[7] L.J. Scott, K.L. Goa, Galantamine: a review of its use in Alzheimer's disease, Drugs 60 (2000) 1095–1122.
[8] M.D. Gottwald, R.I. Rozanski, Rivastigmine, a brain region selective acetylcholinesterase inhibitor for treating Alzheimer's disease: review and current status, Expert Opin. Investig. Drugs 8 (1999) 1673–1682.
[9] G.P. Kumar, F. Khanum, Neuroprotective potential of phytochemicals, Pharmacogn. Rev. 6 (2012) 81–90.
[10] K. Rashed, A.C.C. Sucupira, J.M.M. Neto, et al., Evaluation of acetylcholinesterase inhibition by Alnus rugosa L. stems methanol extract and phytochemical content, Int. J. Biomed. Adv. Res. 4 (2013) 366.
[11] A.G. Atanasov, B. Waltenberger, E.M. Pferschy-Wenzig, et al., Discovery and resupply of pharmacologically active plant-derived natural products: a review, Biotechnol. Adv. 33 (2015) 1582–1614.
[12] L. Ghribia, H. Ghouilaa, A. Omrib, et al., Antioxidant and anti-acetylcholinesterase activities of extracts and secondary metabolites from *Acacia cyanophylla*, Asian Pac. J. Trop. Biomed. 4 (2014) S417–S423.
[13] ⟨http://www.chemspider.com⟩.
[14] ⟨http://www.rcsb.org⟩.
[15] S.K. Tripathi, M. Ravikumar, Sanjeev Kumar Singh, extra precision docking, free energy calculation and molecular dynamics simulation studies of CDK2 inhibitors, J. Theor. Biol. 334 (2013) 87–100.
[16] LigPrep, version 2.5, Schrödinger, LLC, New York, 2011.
[17] K.K. Kakarala, K. Jamil, V. Devaraji, Structure and putative signaling mechanism of protease activated receptor 2 (PAR2)– a promising target for breast cancer, J. Mol. Graph. Model. 53 (2014) 179–199.
[18] Glide, version 5.7, Schrödinger, LLC, New York, 2011.
[19] K.M. Elokely, R.J. Doerksen, Docking challenge: protein sampling and molecular docking performance, J. Chem. Inf. Model. 53 (2013) 1934–1945.
[20] T.A. Binkowski, W. Jiang, B. Roux, et al., Virtual high-throughput ligand screening, Methods Mol. Biol. 1140 (2014) 251–261.
[21] X.Y. Meng, H.X. Zhang, M. Mezei, et al., Molecular docking: a powerful approach for structure-based drug discovery, Curr. Comput. Aid. Drug Des. 7 (2011) 146–157.
[22] Desmond, version 3.0, Schrödinger, LLC, New York, 2011.
[23] J.J. Blessy, D.J. Sharmila, Molecular simulation of N-acetylneuraminic acid analogs and molecular dynamics studies of cholera toxin-Neu5Gc complex, J. Biomol. Struct. Dyn. 33 (2015) 1126–1139.
[24] W.L. Jorgensen, D.S. Maxwell, J.T. Rives, Development and testing of the OPLS All-atom force field on conformational energetics and properties of organic liquids, Am. Chem. Soc. 118 (1996) 11225–11236.
[25] N. Nagasundaram, H. Zhu, J. Liu, et al., Analysing the effect of mutation on protein punction and discovering potential inhibitors of CDK4: molecular modelling and dynamics studies, PLoS One 8 (2015) e0133969.
[26] Prime, version 2.1, Schrödinger, LLC, New York, 2011.
[27] J.M. Hayes, G. Archontis, MM-GB(PB)SA calculations of protein-ligand binding free energies, molecular dynamics - studies of synthetic and biological macromolecules, L. Wang (Ed.), InTech, DOI: http://dx.doi.org/10.5772/37107.
[28] K.K. Kakarala, K. Jamil, Protease activated receptor-2 (PAR2): possible target of phytochemicals, J. Biomol. Struct. Dyn. 33 (2015) 2003–2022.
[29] M.S. Lee, M.A. Olson, Comparison of volume and surface area non polar solvation free energy terms for implicit solvent simulations, J. Chem. Phys. 139 (2013) 044119.
[30] T. Katsila, G.A. Spyroulias, G.P. Patrinos, et al., Computational approaches in target identification and drug discovery, Comput. Struct. Biotechnol. J. 14 (2016) 177–184.
[31] QikProp, version 4.3, Schrödinger, LLC, New York, 2014.
[32] F. Ntie-Kang, L.L. Lifongo, J.A. Mbah, et al., In silico drug metabolism and pharmacokinetic profiles of natural products from medicinal plants in the Congo basin, In Silico Pharmacol. (2013), <http://dx.doi.org/10.1186/2193-9616-1-12>.
[33] A. Ganeshpurkar, A.K. Saluja, The pharmacological potential of rutin, Saudi Pharm. J. 25 (2017) 149–164.
[34] S. Subhani, A. Jayaraman, K. Jamil, Homology modelling and molecular docking of MDR1 with chemotherapeutic agents in non-small cell lung cancer, Biomed. Pharm. 71 (2015) 37–45.
[35] J. Sharma, K. Ramanathan, R. Sethumadhavan, Identification of potential inhibitors against acetylcholinesterase associated with alzheimer's diseases: a molecular docking approach, J. Comput. Method Mol. Des. 1 (2011) 44–51.
[36] S. Roy, A. Kumar, M.H. Baig, et al., Virtual screening, ADMET profiling, molecular docking and dynamics approaches to search for potent selective natural molecules based inhibitors against metallothionein-III to study Alzheimer's disease, Methods 83 (2015) 105–110.
[37] C. Remya, K.V. Dileep, I. Tintu, et al., Flavanone glycosidesas acetylcholinesterase inhibitors: computational and experimental evidence, Indian J. Pharm. Sci. 76 (2014) 567–570.
[38] V. Kuntic, I. Filipović, Z. Vujić, Effects of rutin and hesperidin and their Al (III) and Cu (II) complexes on *in vitro* plasma coagulation assays, Molecule 16 (2011) 1378–1388.
[39] K. Murata, S. Takano, M. Masuda, et al., Anti-degranulating activity in rat basophil leukemia *R*BL-2H3 cells of flavanone glycosides and their aglycones in citrus fruits, J. Nat. Med. 67 (2013) 643–646.
[40] A. Shruthika Ravel, S. Jency, QSAR and docking studies on phytocompounds as lead molecule against Alzheimer's disease, Int. J. Curr. Res. 5 (2013) 1198–1201.